



## Ground gamma-ray survey of the Solforata gas discharge area, Alban Hills-Italy: A comparison between field and laboratory measurements

Federico Di Paolo<sup>a</sup>, Wolfgang Plastino<sup>a,b,\*</sup>, Pavel P. Povinec<sup>c</sup>, Francesco Bella<sup>a</sup>, Antonio Budano<sup>b</sup>, Mario De Vincenzi<sup>a,b</sup>, Matthias Laubenstein<sup>d</sup>, Federico Ruggieri<sup>b</sup>

<sup>a</sup> Department of Physics, University of Roma Tre, Via della Vasca Navale 84, I-00146 Roma, Italy

<sup>b</sup> INFN, Section of Roma Tre, Via della Vasca Navale 84, I-00146 Roma, Italy

<sup>c</sup> Department of Nuclear Physics and Biophysics, Comenius University, Mlynska dolina F-1, SK-84248 Bratislava, Slovakia

<sup>d</sup> INFN, Gran Sasso National Laboratory, S.S. 17 BIS km 18.910, I-67010 Assergi, Italy

### ARTICLE INFO

#### Article history:

Received 9 September 2011

Received in revised form

22 June 2012

Accepted 2 August 2012

Available online 14 September 2012

#### Keywords:

*In situ* gamma-ray survey

HPGe detector

Natural radionuclides

Radon

Solforata gas discharge area

### ABSTRACT

Measurements of environmental radioactivity by HPGe gamma-spectrometry were carried out with the aim of investigating the distribution of natural radionuclides in a volcanic area and to compare two different methodologies – an *in situ* gamma-survey of the area and high accuracy laboratory measurements of soil samples. Results demonstrate good performance of the *in situ* technique, also confirmed by a correlation analysis between the results obtained by the two methodologies. A volcanic gas discharge area was chosen as the test site for the presence of natural long-lived radionuclides such as <sup>40</sup>K and <sup>238</sup>U, <sup>235</sup>U and <sup>232</sup>Th, and their decay chain members. Clear evidence of <sup>222</sup>Rn degassing in the area was confirmed by <sup>226</sup>Ra values measured by the *in situ* technique. Higher <sup>40</sup>K values measured by the *in situ* technique may be attributed to the presence of vegetation in the study area.

© 2012 Elsevier Ltd. All rights reserved.

## 1. Introduction

Natural radioactivity in the environment is mainly produced by long-lived radionuclides such as <sup>40</sup>K and <sup>238</sup>U, <sup>235</sup>U and <sup>232</sup>Th decay chain daughters. The activity of these elements in soils is well documented (UNSCEAR, 2000), and they represent one of the main sources of the lithospheric thermal budget.

*In situ* radiometric surveys of the distribution of natural radionuclides in soil have been a standard technique used either for radioecological investigations or for geophysics studies (Tyler, 2004; Perrin et al., 2006; van der Graaf et al., 2007). As HPGe detectors with electrical cooling have become commercially available, they have replaced previously utilized NaI(Tl) detectors which suffered a low energy resolution which, in environments with multiple gamma-ray sources, caused problems in quantitative high resolution analysis of radionuclides (Povinec et al., 1996).

Some of the Italian volcanic sites have already been investigated using the *in situ* techniques (Chiozzi et al., 2003, 2007), as well as

laboratory analyses (Bellia et al., 1997). However, no detailed *in situ* radiometrics surveys have been carried out in parallel with systematic laboratory comparisons.

The aim of the present study has been to investigate the distribution of natural radionuclides in a geologically active area using *in situ* field gamma-spectrometric survey and laboratory analyses of soil samples. We chose as the test site the Solforata of Pomezia, a volcanic gas discharge area located south of Rome. The results obtained by a direct *in situ* activity measurement are compared with laboratory analysis of soil samples. In both cases gamma-spectrometry with HPGe detectors was chosen as the best compromise between the high energy resolution and reasonable detection efficiency for gamma-ray emitters. Preliminary results of these investigations have been published by Di Paolo et al. (2011).

## 2. Samples and analytical methods

### 2.1. Geological setting

The Solforata of Pomezia is a gaseous discharge area located 8 km south of Rome, on the southwestern flank of the Alban Hills volcanic complex. The site lies on a flood valley which crosses the

\* Corresponding author. Department of Physics, University of Roma Tre, Via della Vasca Navale 84, I-00146 Roma, Italy. Tel.: +39 0 657337277; fax: +39 0 657337102.  
E-mail address: [plastino@fis.uniroma3.it](mailto:plastino@fis.uniroma3.it) (W. Plastino).

overlapping products of the III and VI pyroclastic eruptions of Tuscolano-Artemisio phase (De Rita et al., 1988). The Alban Hills complex has been subject to volcanic activity from about 600 to 20 ky BP, with three eruptive phases (De Rita et al., 1995). The first one, Tuscolano-Artemisio phase between 600 and 300 ky BP, was the most intense and ended with a collapse leaving a 10 km wide caldera. The second, Faete phase between 300 and 200 ky BP, was characterized by postcalderic scoria cones, strombolian activity and large extrusions forming the Faete edifice. The last phase, from 200 to 20 ky BP was mainly hydromagmatic, concentrated on the western flank of the volcano. During the whole eruptive story, pyroclastic flows covered an area of about 1500 km<sup>2</sup> (Chiodini and Frondini, 2001). The most recent phenomena related to the presence of magma are low-magnitude seismic swarms and uplift close to the Albano Lake on the western side of the complex (Amato and Chiarabba, 1995).

Solforata is located close to a subsiding area bordered by a complex fault system called *Ardea fault zone*. This is a 30–40 km long and 10 km wide half-graben structure bordered by 40°N normal faults with a roll-over structure on the hanging wall, crossing an NW-SE fault system (De Rita et al., 1995). The spatial distribution of scoria cones of the last eruptive phase of the volcanic complex is clearly aligned along these faults.

Related to this fault system, the site shows some of the most intense degassing in the Alban Hills area. The presence of exhalations in the Solforata has been historically well known since the Roman age. In 1877 an intense CO<sub>2</sub> discharge occurred in coincidence with an earthquake localized nearby (Funciello et al., 2002). During this period other similar instantaneous degassing events occurred, showing a relationship between fracturing processes and gas emissions. The active fault system in the Alban Hills area, and especially in the Solforata site, represents the main path for gases released from the geothermic reservoir to reach the surface.

At present, the degassing at Solforata (both in terrain and water) is well documented (Giggenbach et al., 1988; Chiodini and Frondini, 2001; Voltaggio et al., 2001; Voltaggio and Spadoni, 2009). The gases consist mainly of CO<sub>2</sub>, with minor amounts of H<sub>2</sub>S, <sup>222</sup>Rn and

N<sub>2</sub>. Chiodini and Frondini (2001) measured a mean CO<sub>2</sub> release of  $4.62 \times 10^7$  g/day. Voltaggio and Spadoni (2009) measured in spring 2007 a H<sub>2</sub>S flux of about 1208 kg/day. Voltaggio et al. (2001) reported a mean activity concentration of <sup>222</sup>Rn in the effluents of 150,000 Bq/m<sup>3</sup>. Voltaggio and Spadoni (2009) reported H<sub>2</sub>S concentrations in terrain exceeding 30 ppmv nearby the main pool of the Solforata; sulphur is abundant in this zone and a mine was active until 30–40 years ago. The intense emission of acid gases is also demonstrated by the absence of vegetation in the area and bubbling inside the pool. Water temperature is low, about 20 °C, but a value of about 50 °C was reached at Pozzo CO.MI.RO (near Solforata pools) during the 1981 seismic crisis (Calcarà et al., 1995).

The presence of sulphur in water and gases seems to be connected with a deep source. Cavarretta and Lombardi (1992) suggested, on the basis of salinity and sulphur isotope data, that the water discharge in the volcanic and perivolcanic areas of Latium has two components: meteoric water circulating and interacting with the carbonate basement which is mixed with a deep component rich in gas, rising along the major regional tectonic lineaments.

## 2.2. Sampling methodology

Sampling points at the Solforata gas discharge area were chosen from satellite images and aerial photographs. We considered as the main area of the investigation the zone around the pools (where the most intense degassing vents are located). Two other study areas were located nearby. Three square grids with side length of 50 m were designed using a Geographic Information System (GIS). Once in the field, using a GPS we were able to reach the centre of each square. We were not able to reach many sampling points because of the roughness of the terrain. Fig. 1 depicts all sampling points. Altogether 47 soil samples were collected Fig. 2 shows the isolines of altitude above sea level (m a.s.l.) with sampling points.

Area 1 is located on a hill NW of the pools, with steep slopes. At the time of survey it was completely covered by vegetation, showing a clear absence of degassing. 15 soil samples were collected in this area.

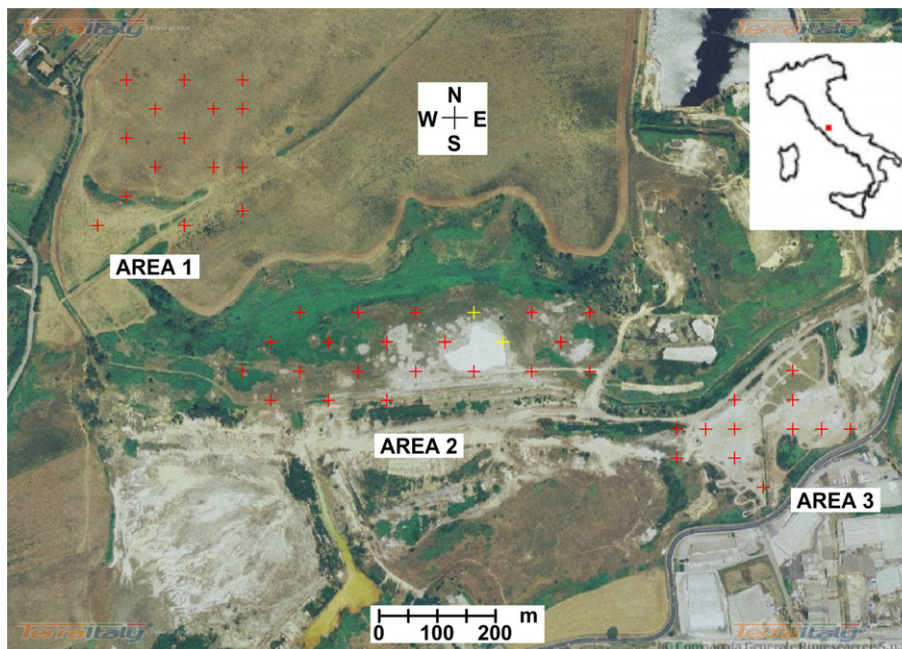


Fig. 1. Sampling points for both *in situ* and laboratory measurements (in red), and for *in situ* measurements only (in yellow). (For interpretation of the references to colour in this figure legend, the reader is referred to the web version of this article.)

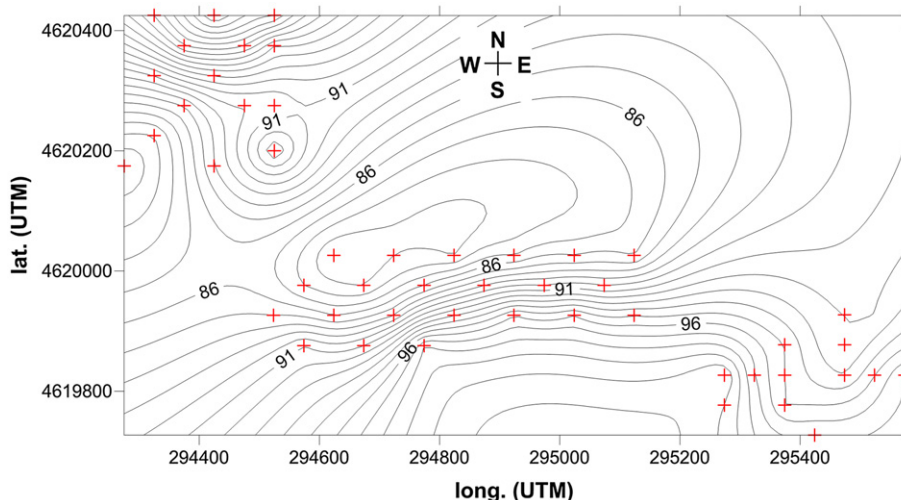


Fig. 2. Contour isoline maps for the altitude (m a.s.l.).

Area 2 is the main area of investigation, located in a valley with pools. The main pool has a maximum elongation of 100 m. At the time of measurements (April 2008) there was a smaller pool nearby with radius of about 3 m. In this area it was possible to collect 20 samples with uniform spacing between them, thanks to the gentle topography. The intense degassing in this area is clearly visible inside the pools (where bubbling is evident) and all around, because of the absence of vegetation. Water temperature in the pools is low, close to the atmospheric value.

Area 3 is located nearby a road which provides the only entrance to the Solforata. The area is extremely arid, and the terrain is so rough that it was not possible to reach many sampling points of the grid. No degassing was observed inside this area. A number of 12 soil samples were collected in this area.

As the most of crust radiation comes from a thin layer of soil (IAEA, 2003) we collected samples down to a depth of 20 cm, taking care to collect no vegetation so only measurements of soil activity were carried out. To avoid any contamination between samples, these were stored in two nylon sacks and after sampling each tool was cleaned well. Masses of collected samples were around 1 kg.

2.3. Field measurements

The *in situ* measurements were carried out with a hand-held ORTEC DETECTIVE-EX-100 portable gamma-spectrometer housing an HPGe detector with a *p*-type closed-end coaxial crystal of 181 cm<sup>3</sup> volume and a detection efficiency of 76% relative to

a 3" × 3" NaI(Tl) detector. The detector crystal was maintained at a temperature of 100 K by an electrical cooling system (Keyser et al., 2005a, 2005b; Twomey and Keyser, 2005). An 8192 channel Multi Channel Analyzer (MCA) integrated inside the spectrometer provided energy resolution in the energy range of 0–3000 keV of about 0.37 keV. ORTEC-GammaVision 6.07 software was used for data acquisition.

The energy and efficiency calibration of the detector was carried out using point sources of known activity (<sup>133</sup>Ba, <sup>57</sup>Co, <sup>137</sup>Cs, <sup>54</sup>Mn), positioned at a distance of 25 cm from the endcap of the detector. The energy curve shows good linearity, with the quadratic term six orders of magnitude lower than the linear term:

$$E(\text{ch}) = 0.43 \cdot \text{ch} + 2.14 \cdot 10^{-7} \cdot \text{ch}^2 \tag{1}$$

The measurements of radioactive sources were combined with numerical simulations using the GEANT4 code (Agostinelli et al., 2003).

Once in the field, the detector was positioned in order to have the crystal at a height of 1 m from the soil. To obtain good statistics during the ground survey, we chose 2 min of counting time for each measurement point. Natural radioactivity is usually associated with the decay of long-lived members of the radioactive chains of <sup>238</sup>U, <sup>235</sup>U and <sup>232</sup>Th, and with the 1460.82 keV gamma-line of <sup>40</sup>K. The <sup>238</sup>U, <sup>235</sup>U and <sup>232</sup>Th decay chains contain many gamma-emitters with different decay energies. We chose some of these, on the basis of three conditions:

- (i) in order to have good counting statistics we chose the lines with the highest emission probabilities.
- (ii) for better discrimination between two emitters we discarded peaks which were too close to resolve clearly.
- (iii) we discarded low-energy gamma-lines because of high contribution of Compton scattering.

The characteristics of the gamma-lines chosen for the analysis are given in Table 1. Assuming a secular equilibrium, activities of

Table 1  
Lines of gamma emission chosen both for field and laboratory analysis.

Radionuclide	Energy (keV)	E.P. <sup>a</sup>
<sup>235</sup> U <sup>b</sup>	185.71	0.57
<sup>214</sup> Pb	351.93	0.35
<sup>214</sup> Bi	609.32	0.47
	1764.50	0.16
<sup>234m</sup> Pa <sup>b</sup>	1001.02	0.01
<sup>228</sup> Ac	911.32	0.29
	964.77	0.06
	968.97	0.17
<sup>212</sup> Pb	288.63	0.44
<sup>208</sup> Tl	583.19	0.85
	2614.55	0.99
<sup>40</sup> K	1460.82	0.11

<sup>a</sup> Emission probability.  
<sup>b</sup> Not visible for spectra acquired in field.

Table 2  
Background levels for the detectors used in the laboratory analysis.

Detector	Total background and several radionuclides (counts/day)			
	(60–2700) keV	<sup>214</sup> Bi (352 keV)	<sup>208</sup> Tl (583 keV)	<sup>40</sup> K (1461 keV)
GsOr	980	5.1	1.7	8.4
GePV	951	5.3	4.1	6.3

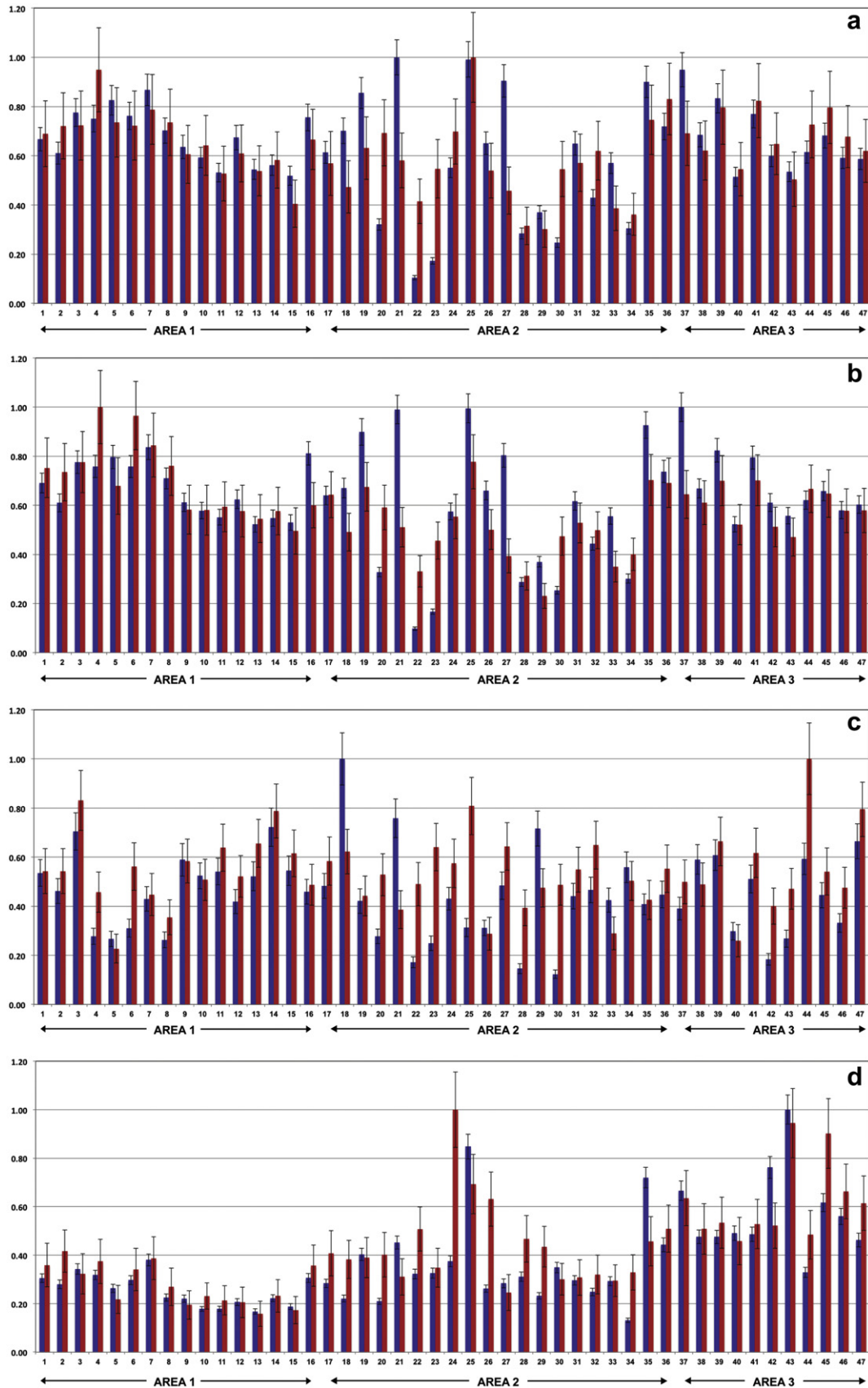


**Fig. 3.** Scatter graph of surface activity ( $\text{Bq m}^{-2}$ ) for both the techniques: laboratory analysis (blue) and field survey (red). Values are normalized to make clear the correlation between the two methods. a:  $^{228}\text{Ra}$ , b:  $^{228}\text{Th}$ , c:  $^{40}\text{K}$ , d:  $^{226}\text{Ra}$ . (For interpretation of the references to colour in this figure legend, the reader is referred to the web version of this article.)

long-lived radionuclides were calculated by weighting the single activities of their daughters with the variance:

$$A = \frac{\sum_{i=1}^n A_i / \sigma_i^2}{\sum_{i=1}^n 1 / \sigma_i^2} \quad (2)$$

For example, the activity of  $^{226}\text{Ra}$  was calculated from the activities of  $^{214}\text{Pb}$  and  $^{214}\text{Bi}$ . The same procedure was used for the calculation of  $^{228}\text{Ra}$  activity from  $^{228}\text{Ac}$ , and  $^{228}\text{Th}$  from  $^{208}\text{Tl}$  and  $^{212}\text{Pb}$ .

#### 2.4. Laboratory analysis

The analysis of soil samples was performed by gamma-spectrometry at the Laboratori Nazionali del Gran Sasso (LNGS). This is an underground laboratory located near the city of L'Aquila (Italy) beneath 1400 m of rock. The effect of rock overburden surrounding the laboratory corresponds to 3800 water equivalent (m w.e.), making the LNGS a very low background facility for measurements of very low activity samples (Laubenstein et al., 2004).

The counting facility (Laboratorio di Radiopurezza) is equipped with nine *p*-type HPGe detectors of coaxial configuration; two of these were used for the analysis of soil samples. Detector GsOr has a volume of 403 cm<sup>3</sup> with an efficiency of 96%. Detector GePv has a volume of 363 cm<sup>3</sup> with an efficiency of 91%. The detection efficiencies are relative to a 3" × 3" NaI(Tl) detector. Both detectors have a Full Width at Half Maximum of 1.9 keV for the full energy peak at 1332.47 keV for  $^{60}\text{Co}$ . Each detector is shielded by 25 cm of low activity lead with intrinsic  $^{210}\text{Pb}$  activity below 20 Bq/kg. In order to stop the X-rays and bremsstrahlung produced from lead, there is an inner shielding made of 10 cm thick high conductivity oxygen free copper. A further reduction of neutron flux is obtained by shielding the detectors from the bottom with 5 cm of acrylic and cadmium foil (Arpesella, 1996). A plastic cover surrounding the whole shielding system is continuously flushed with nitrogen gas to reduce radon contamination. A ventilation system already

reduces the radon content in the laboratory, maintaining an activity concentration of  $^{222}\text{Rn}$  of about 30 Bq/m<sup>3</sup>. The entire shielding together with the rock overburden reduces the background radioactivity by a factor of two with respect to a similar laboratory situated at the surface. Table 2 shows the intrinsic background levels for each detector. The main contributions are from  $^{40}\text{K}$  and  $^{208}\text{Tl}$  ( $^{232}\text{Th}$  daughter), showing counting rates of about 0.4 h<sup>-1</sup>, considerably below counting rates from the soil samples analysed in this study.

The HPGe detectors were calibrated using a  $^{60}\text{Co}$  standard source of known activity with the main gamma-emissions at 1173.21 and 1332.47 keV. The amplifier gain was fixed in order to fully cover the range of 8192 channels (30–3500 keV) of the MCA over the energy range typical for gamma-emissions from natural radionuclides (Di Paolo et al., 2011). Counting time was a function of sample mass, activity concentration and geometry of samples, and varied from a minimum of half an hour to several hours. The uncertainties associated with measured activity values depend on many factors: the accuracy of efficiency calibration (about 5%), sample composition and density, geometry and (for very low concentrations) the statistical uncertainty of the counting. The efficiency calibration was carried out using the GEANT4 code (Agostinelli et al., 2003), that accurately reproduces the characteristics of detectors.

The soil samples were placed during analyses inside Marinelli beakers, which helped to maximize the detection efficiency. The sample masses varied between 0.3 and 1 kg. In order to maintain measurement conditions similar to those during the field surveys, no chemical treatments were performed on soil samples. Gamma-lines used for the radionuclide analyses were the same as those used during the field surveys. During the laboratory measurements we were also able to analyse gamma-lines from  $^{234\text{m}}\text{Pa}$  and  $^{235}\text{U}$ .

### 3. Results and discussion

Fig. 3 shows results of measurements obtained from both the field survey (with typical uncertainties between 15 and 25%) and

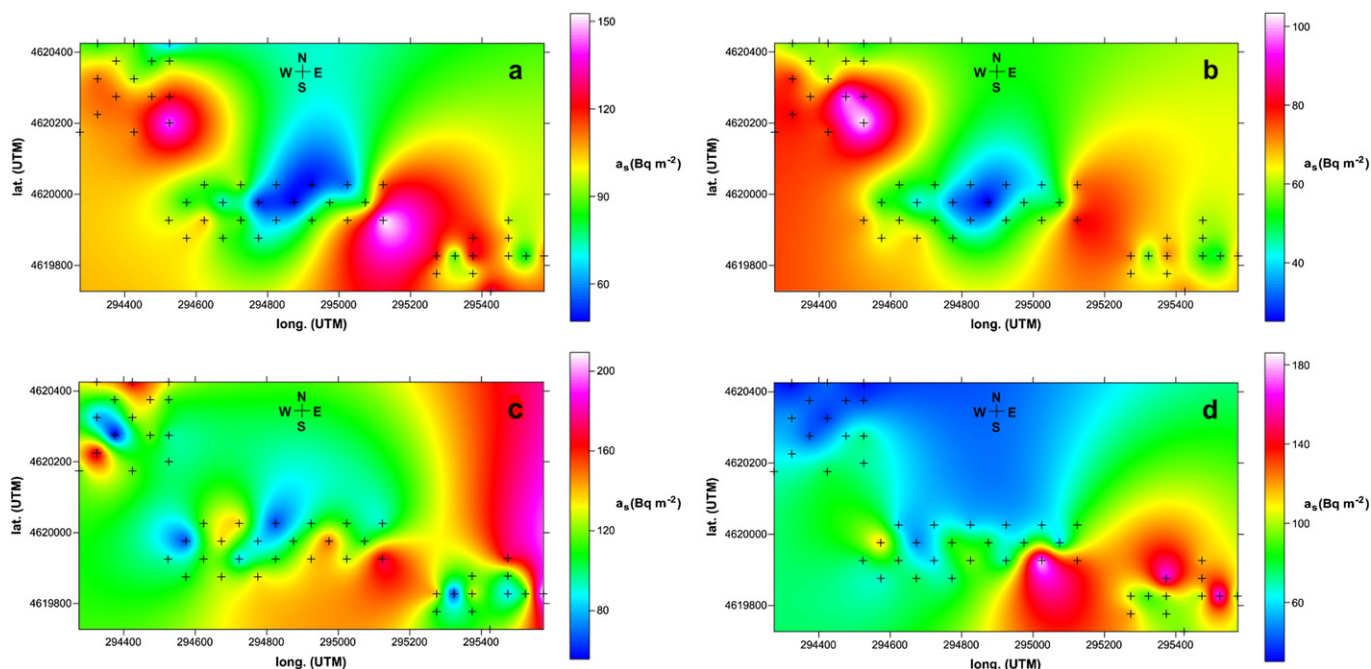


Fig. 4. Surface activity (Bq m<sup>-2</sup>) maps obtained from *in situ* measurements. a:  $^{228}\text{Ra}$ , b:  $^{228}\text{Th}$ , c:  $^{40}\text{K}$ , d:  $^{226}\text{Ra}$ .

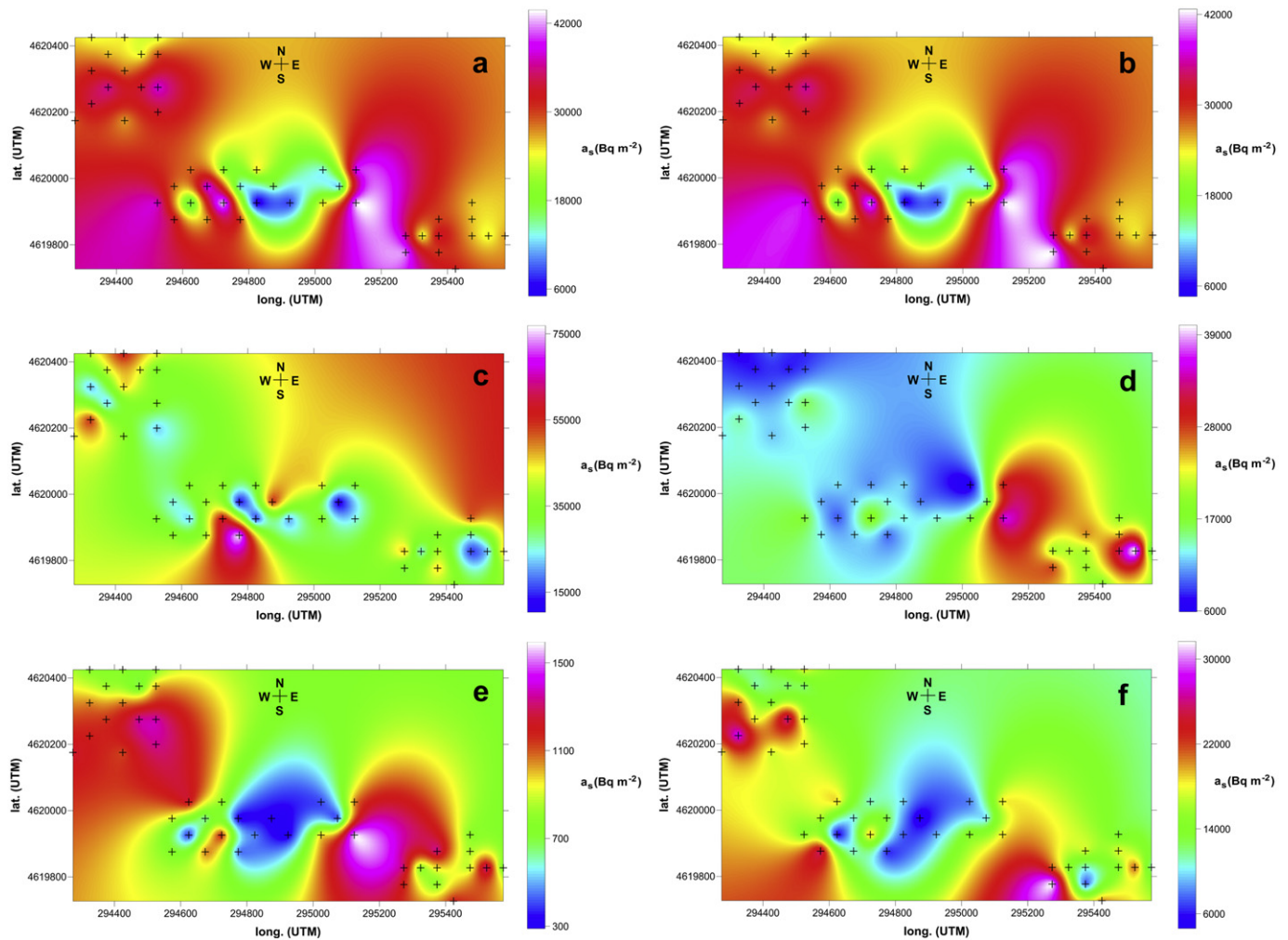


Fig. 5. Surface activity ( $\text{Bq m}^{-2}$ ) maps obtained from laboratory analysis of soil samples. a:  $^{228}\text{Ra}$ , b:  $^{228}\text{Th}$ , c:  $^{40}\text{K}$ , d:  $^{226}\text{Ra}$ , e:  $^{235}\text{U}$ , f:  $^{234\text{m}}\text{Pa}$ .

the results of laboratory analyses (with uncertainties between 6 and 13%). The lower uncertainties obtained in the laboratory are typical for low-background counting conditions when compared with the field measurements. High uncertainties associated with  $^{137}\text{Cs}$  are due to its very low content in soil samples.

Surface activity maps for natural radionuclides obtained from field surveys are shown in Fig. 4 with sampling points indicated as crosses. Fig. 5 shows maps of surface activity of soil samples for natural radionuclides obtained from laboratory analyses. Interpolations were made using the kriging method. The presence of

anthropogenic  $^{137}\text{Cs}$  was detected inside Area 2, near the degassing pools. Fig. 6 shows activity maps of  $^{137}\text{Cs}$  inside Area 2 obtained using both methodologies. Table 3 lists correlation coefficients between the results obtained with the two methodologies.

The surface activity maps obtained from direct *in situ* gamma-spectrometry measurements carried out in the field (Fig. 4) show values comparable for all radionuclides. The  $^{40}\text{K}$  is more abundant, with values ranging between  $48.7 \text{ Bq m}^{-2}$  and  $214 \text{ Bq m}^{-2}$  (av.  $116.50 \text{ Bq m}^{-2}$ ),  $^{226}\text{Ra}$  activity varies from  $29.7 \text{ Bq m}^{-2}$  to  $188 \text{ Bq m}^{-2}$  (av.  $79.4 \text{ Bq m}^{-2}$ ). Neither radionuclide shows any

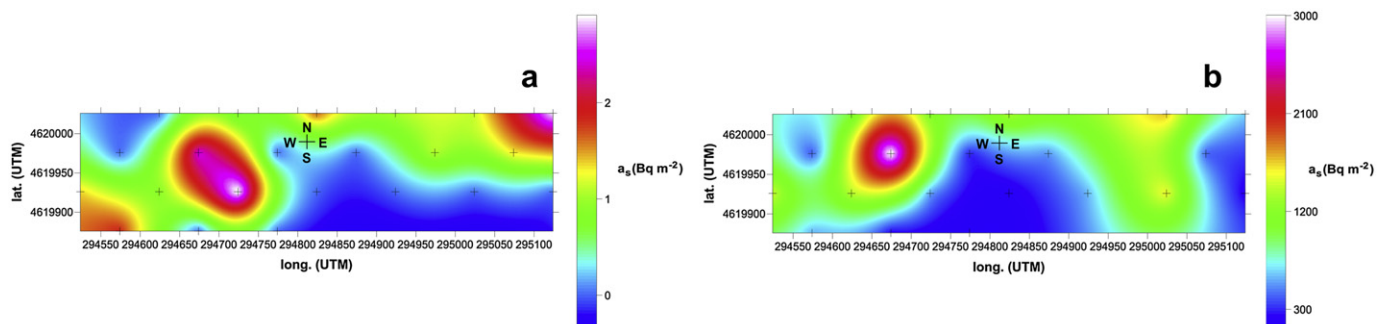


Fig. 6. Surface activity ( $\text{Bq m}^{-2}$ ) maps of  $^{137}\text{Cs}$  in area 2 from *in situ* measurements (a) and measured in the laboratory (b).

**Table 3**Correlation coefficients (*R*) between the results from the *in situ* and laboratory measurements.

	Area 1 (15 pts)	Area 2 (20 pts)	Area 3 (12 pts)	Total (47 pts)
$^{226}\text{Ra}$	0.85	0.35	0.70	0.71
$^{228}\text{Ra}$	0.79	0.52	0.61	0.59
$^{228}\text{Th}$	0.80	0.65	0.67	0.62
$^{40}\text{K}$	0.86	0.08	0.75	0.46
$^{137}\text{Cs}$	–	0.43	–	–
<i>R</i> (5%)	0.51	0.44	0.58	0.29
<i>R</i> (1%)	0.64	0.56	0.71	0.37

particular patterns on the maps.  $^{228}\text{Ra}$  varies between  $46.3 \text{ Bq m}^{-2}$  and  $153 \text{ Bq m}^{-2}$  (av  $96.2 \text{ Bq m}^{-2}$ ), and  $^{228}\text{Th}$  varies between 24 and  $104 \text{ Bq m}^{-2}$  (av  $60.9 \text{ Bq m}^{-2}$ ).  $^{228}\text{Ra}$  and  $^{228}\text{Th}$  values are in reasonable agreement, with low activities in the centre of Area 2 (near the main pool), and seem to be in equilibrium.

The surface activity of soil samples obtained by laboratory analysis (Fig. 5) shows clear similarities with the *in situ* measurements.  $^{228}\text{Ra}$  ranges from  $4.59 \text{ kBq m}^{-2}$  to  $44.14 \text{ kBq m}^{-2}$  (av.  $27.68 \text{ kBq m}^{-2}$ ).  $^{228}\text{Th}$  varies between  $4.19 \text{ kBq m}^{-2}$  and  $42.79 \text{ kBq m}^{-2}$ , with an average value of  $26.84 \text{ kBq m}^{-2}$ . These two radionuclide activities are again in good agreement with low values concentrated in the centre of Area 2. The same pattern is visible also for surface activity maps of  $^{234\text{m}}\text{Pa}$  and  $^{235}\text{U}$ , although the activities are much lower because the concentration of the parent radionuclide is much lower than that of  $^{238}\text{U}$  and  $^{232}\text{Th}$ . The  $^{234\text{m}}\text{Pa}$  shows values between  $4.38 \text{ kBq m}^{-2}$  and  $32.30 \text{ kBq m}^{-2}$  (av  $15.06 \text{ kBq m}^{-2}$ ), and  $^{235}\text{U}$  varies between  $280 \text{ Bq m}^{-2}$  and  $1600 \text{ Bq m}^{-2}$  with an average value of  $920 \text{ Bq m}^{-2}$ . The  $^{226}\text{Ra}$  surface activity varies between  $7.06 \text{ kBq m}^{-2}$  and  $42.27 \text{ kBq m}^{-2}$  (av.  $15.65 \text{ kBq m}^{-2}$ ), although its distribution is different from that of  $^{228}\text{Ra}$  and  $^{228}\text{Th}$ .  $^{40}\text{K}$  varies between  $9.60 \text{ kBq m}^{-2}$  and  $78.20 \text{ kBq m}^{-2}$  with an average of  $35.80 \text{ kBq m}^{-2}$ .

The results presented are within ranges reported for other areas in the world (UNSCEAR, 2000). They are also in agreement with measurements reported by other authors, both in the same site (Votaggio et al., 2001), as well as in other Italian volcanic areas (Chiozzi et al., 2003, 2007).

A clear activity minimum is evident for  $^{228}\text{Ra}$ ,  $^{228}\text{Th}$ ,  $^{235}\text{U}$  and  $^{234\text{m}}\text{Pa}$  in Area 2. This is the most interesting result as this area is well known because of intense degassing. Both methodologies show a similar feature, although  $^{226}\text{Ra}$  and  $^{40}\text{K}$  do not show this pattern.

In order to compare the two methodologies, correlation coefficients were calculated (Table 3). A comparison is also shown in Fig. 3. Area 1 presents the highest level of correlation for all radionuclides, with a significance level of 1%. This area was the most uniform, totally covered by vegetation at the time of survey. No degassing was detected in this area. Area 3 also shows a strong correlation for all radionuclides, at a confidence level of 5%. At the time of survey this area was almost totally arid, with absence of degassing. The correlation coefficients in Area 2 confirm a correlation at the 5% confidence level for  $^{228}\text{Ra}$  and  $^{228}\text{Th}$ , but no correlation was found for  $^{40}\text{K}$  and  $^{226}\text{Ra}$ . The intense degassing observed during the field survey, which was also reported by Chiodini and Frondini (2001) and Votaggio et al. (2001) could be a source of this disagreement. In Fig. 7, the ratio of  $^{226}\text{Ra}$  surface activities measured in the field to the soil surface activity measured in the laboratory shows an excess of  $^{226}\text{Ra}$  measured in the field. This result may be explained by a presence of  $^{222}\text{Rn}$  degassing during the field survey. Furthermore, the anomalies are located nearby the main pool, where intense degassing was observed during the survey, and also reported by Votaggio et al. (2001).

The  $^{40}\text{K}$  data for Area 2 did not show any correlation between the two methodologies. This result may be due to an effect of vegetation. As  $^{40}\text{K}$  can be easily transferred from soil to vegetation (Papastefanou et al., 1999; Korobova et al., 2007), it may enlarge  $^{40}\text{K}$  levels measured by the *in situ* methodology. In Area 1 the vegetation cover is almost uniform, so a contribution of  $^{40}\text{K}$  from grass does not alter the spatial distribution of radiation. Area 3 is completely arid, so this effect is not present at all. However, in Area 2 the vegetation cover is not uniform, so  $^{40}\text{K}$  contribution from the vegetation may cause spatial anomalies in the  $^{40}\text{K}$  distribution.

The presence of anthropogenic  $^{137}\text{Cs}$  (Fig. 6) in the study area is probably due to Chernobyl and weapons fallout, and both field and laboratory techniques were able to detect it. Compared to the natural radionuclides these values are rather low, varying in soil samples from  $137.14$  to  $1675 \text{ Bq m}^{-2}$ . *In situ* measurements give a maximum value of  $3 \text{ Bq m}^{-2}$ , however the uncertainties are high (up to 60%). The presence of vegetation can also influence the  $^{137}\text{Cs}$  distribution in the area, as  $^{137}\text{Cs}$  can be easily transferred from soil to plants similarly to  $^{40}\text{K}$  (Papastefanou et al., 1999). Moreover, cesium and potassium are homologous elements and cesium can substitute for potassium in soil and plants (Papastefanou et al., 1988).

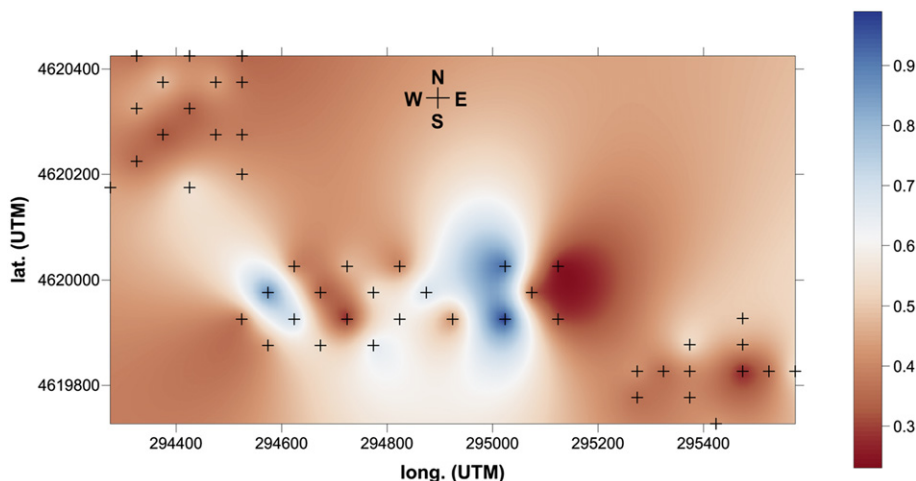


Fig. 7. Ratio of  $^{226}\text{Ra}$  (field)/ $^{226}\text{Ra}$  (laboratory) normalized.

#### 4. Conclusions

Two different methodologies for gamma-spectrometry analysis of soil samples based on laboratory and field measurements were compared with the aim of testing the accuracy of a portable gamma-spectrometer for *in situ* measurements. Because of the short counting time, the surface activities measured in the field are significantly lower than those obtained from the laboratory analysis. Nevertheless the field survey demonstrated the validity of the *in situ* measurements, capable of identifying the same features in the distribution of natural radionuclides and anthropogenic  $^{137}\text{Cs}$  in soil, as observed by high accuracy laboratory gamma-spectrometry measurements.

A volcanic gas discharge area was chosen as the test site for the presence of natural long-lived radionuclides such as  $^{40}\text{K}$  and  $^{238}\text{U}$ ,  $^{235}\text{U}$  and  $^{232}\text{Th}$ , and their decay chain members. Clear evidence of  $^{222}\text{Rn}$  degassing in the area was confirmed by anomalous  $^{226}\text{Ra}$  values measured by the *in situ* technique. A different pattern for  $^{40}\text{K}$  measured by the *in situ* technique may be attributed to the presence of vegetation in the study area. The *in situ* gamma-spectrometer was also able to analyse the distribution of anthropogenic  $^{137}\text{Cs}$  in the study area. The comparison between field and laboratory surveys can also provide a tool to study the distribution of radon and thoron degassed from large soil areas. Numerical simulations are under way to quantify the amount of radon emitted during such field measurements.

#### Acknowledgements

The authors highly acknowledge the support by the National Scientific Committee Technology of INFN for the ERMES project, and the European Commission under the FP7 programme for the EUMEDGRID project (Grant RI-246589). The authors are grateful to the Grid Lab of INFN and the Department of Physics of University of Roma Tre, and specifically to Federico Bitelli. PPP acknowledges a support provided by the Structural Funds of EU – the Research and Development Operational Program funded by the ERDF (project No. 26240220004).

#### References

- Agostinelli, S., et al., 2003. Geant4-A simulation toolkit. Nucl. Instr. Meth. Phys. Res. Sect. A 506, 250–303.
- Amato, A., Chiarabba, C., 1995. Recent uplift of the Alban hills volcano (Italy): evidence for a magmatic inflation? Geophys. Res. Lett. 22, 1985–1988.
- Arpesella, C., 1996. A low background counting facility at laboratori Nazionali del Gran Sasso. Appl. Radiat. Isot. 47, 991–996.
- Bellia, S., Brai, M., Hauser, S., Puccio, P., Rizzo, S., 1997. Natural radioactivity in a volcanic Island: Ustica, Southern Italy. Appl. Radiat. Isot. 48 (2), 87–293.
- Calcara, M., Lombardi, S., Quattrocchi, F., 1995. Geochemical monitoring for seismic surveillance. In: Trigila, R. (Ed.), The Volcano of the Alban Hills, Rome, pp. 243–265.
- Cavarretta, G., Lombardi, G., 1992. Origin of sulphur in minerals and fluids from Latium (Italy): isotopic constraints. Eur. J. Mineral. 4, 1311–1329.
- Chiodini, G., Frondini, F., 2001. Carbon dioxide degassing from the Albani Hills volcanic region, Central Italy. Chem. Geol. 177, 67–83.
- Chiozzi, P., Pasquale, V., Verdoya, M., Minato, S., 2003. Gamma-ray activity in the volcanic islands of the Southern Tyrrhenian Sea. J. Environ. Radioact. 67, 235–246.
- Chiozzi, P., Pasquale, V., Verdoya, M., 2007. Radiometric survey for exploration of hydrothermal alteration in a volcanic area. J. Geoch. Expl. 93, 13–20.
- De Rita, D., Funiello, R., Parotto, M., 1988. Carta Geologica del Complesso Vulcanico dei Colli Albani. CNR, Rome.
- De Rita, D., Faccenna, C., Funiello, R., Rosa, C., 1995. Stratigraphy and volcano-tectonics. In: Trigila, R. (Ed.), The Volcano of the Alban Hills, Rome, pp. 33–66.
- Di Paolo, F., Plastino, W., Povinec, P.P., Bella, F., Budano, A., De Vincenzi, M., Laubenstein, M., Ruggieri, F., 2011. Ground Gamma Ray Survey by HPGe: Numerical Simulations and Comparison Between Field and Laboratory Measurements. Seventh International Conference on Natural Computation, vol. 4, IEEE, Shanghai, pp. 2129–2132.
- Funiello, R., Giordano, G., De Rita, D., Carapezza, M.L., Barberi, F., 2002. L'attività recente del cratere del Lago Albano di Castelgandolfo. Rend. Fis. Acc. Lincei. 9, 113–114.
- Giggenbach, W.F., Minissale, A.A., Scandiffo, G., 1988. Isotopic and chemical assessment of geothermal potential of the Colli Albani area, Latium region, Italy. Appl. Geochem. 3, 475–486.
- IAEA, 2003. Guidelines for Radioelement Mapping Using Gamma Ray Spectrometry Data. IAEA Technical Documents. [http://www-pub.iaea.org/MTCD/publications/PDF/te\\_1363\\_web.pdf](http://www-pub.iaea.org/MTCD/publications/PDF/te_1363_web.pdf).
- Keyser, R.M., Twomey, T.R., Upp, D.L., 2005a. An Improved Handheld Radioisotope Identifier (RID) for Both Locating and Identifying Radioactive Materials. HPS Midyear. <http://www.ortec-online.com/Library/index.aspx?tab=2>.
- Keyser, R.M., Twomey, T.R., Upp, D.L., 2005b. A Comparison of an HPGe-based and NaI-based Radionuclide Identifier (RID) for Radioactive Materials. ESARDA. <http://www.ortec-online.com/Library/index.aspx?tab=2>.
- Korobova, E.M., Brown, J.B., Ukrainseva, N.G., Surkov, V.V., 2007.  $^{137}\text{Cs}$  and  $^{40}\text{K}$  in the terrestrial vegetation of the Yenisey Estuary – landscape, soil and plant relationships. J. Environ. Radioact. 96, 144–156.
- Laubenstein, M., Hult, M., Gasparro, J., Arnold, D., et al., 2004. Underground measurements of radioactivity. Appl. Rad. Isot. 61, 167–172.
- Papastefanou, C., Manolopoulou, M., Charalambous, S., 1988. Cesium-137 in soils from Chernobyl fallout. Health Phys. 55, 985–987.
- Papastefanou, C., Manolopoulou, M., Stoulos, S., Ioannidou, A., Gerasopoulos, E., 1999. Soil-to-plant transfer of  $^{137}\text{Cs}$ ,  $^{40}\text{K}$  and  $^7\text{Be}$ . J. Environ. Radioact. 4, 59–65.
- Perrin, J., Carriera, F., Guillot, L., 2006. Determination of the vertical distribution of radioelements (K, U, Th, Cs) in soils from portable HP-Ge spectrometer measurements: a tool for soil erosion studies. Appl. Rad. Isot. 64, 830–843.
- Povinec, P.P., Osvath, I., Baxter, M.S., 1996. Underwater gamma-spectrometry with HPGe and NaI(Tl) detectors. Appl. Radiat. Isot. 47, 1127–1133.
- Tyler, A.N., 2004. High accuracy in situ radiometric mapping. J. Environ. Radioact. 72, 195–202.
- Twomey, T.R., Keyser, R.M., 2005. A New, Portable High-resolution Gamma-ray Instrument for Use in On-site Safeguards Inspection. JRC Workshop. <http://www.ortec-online.com/Library/index.aspx?tab=2>.
- UNSCEAR, 2000. Sources and Effects of Ionizing Radiations. (Report to the General Assembly with Scientific Annexes. United Nations, New York).
- van der Graaf, E.R., Koomansb, R.L., Limburgb, J., de Vriesb, K., 2007. In situ radiometric mapping as a proxy of sediment contamination: assessment of the underlying geochemical and -physical principles. Appl. Rad. Isot. 65, 619–633.
- Voltaggio, M., Di Lisa, G.A., Voltaggio, S., 2001. U-series disequilibrium study on a gaseous discharge area (Solforata of Pomezia, Alban Hills, Italy): implications for volcanic and geochemical risk. Appl. Geochem. 16, 57–72.
- Voltaggio, M., Spadoni, M., 2009. Mapping of H<sub>2</sub>S fluxes from the ground using copper passive samplers: an application study at the Solforata di Pomezia degassing area (Alban Hills, Central Italy). J. Volcanol. Geotherm. Res. 179, 56–68.